Dalton Transactions

Accepted Manuscript

ROYAL SOCIETY OF CHEMISTRY

www.rsc.org/dalton

A Zwitterionic Triphosphenium Compound as a Tunable Multifunctional Donor

Received 00th January 20xx,
Accepted 00th January 20xx

DOI: 10.1039/x0xx00000x

www.rsc.org/

Stephanie C. Kosnik, and Charles L. B. Macdonald*

The preparation of a novel triphosphenium zwitterion featuring di-, tri-, and tetra-coordinate phosphorus centres derived from a 1,2,4-tris-(diphenylphoshinyl)cyclopentadienyl framework is described. The reactivity of this potentially multidentate donor with protons, elemental sulfur and gold(I) chloride is examined, and the preferential reactivity of the pendant phosphine group over the P(I) centre is rationalized on the basis of density functional theory investigations.

Introduction

It is understood that main group chemistry has undergone a renaissance within the last two decades.[1] One of the principal areas of investigation during this time has been the development of stable compounds containing elements in low valence states or low oxidation states.[2] A landmark class of molecules containing low-valent phosphorus atoms are the triphosphenium cations, which are stable molecules containing a dicoordinate phosphorus atom in the +1 oxidation state, stabilized by two phosphonio substitutents.[3,4] Because of the electron-rich nature of the P^I fragment, these molecules were initially proposed to be good candidates for coordination chemistry as ligands for transition metals. However, in spite several reports of improved syntheses[5,6] and some reports of complex formation,[7] the coordination chemistry of these molecules remains underdeveloped – particularly in comparison to their isoelectronic carbon(0) analogues known as carbodiphosphoranes.[8–11] The relatively poor ligating ability of triphosphenium cations is likely a consequence of the positive charge on the moiety containing the P^I center in addition to the presence of reactive anions. For example, it has been postulated that the bromide ion of (Fig. 1, A) preferentially reacts with transition metals, leading to degradation of the triphosphenium fragment.[12] To overcome these deficiencies, Ragogna and co-workers recently reported a zwitterionic cyclic triphosphenium species – constructed using anionic phosphine ligands – and demonstrated that the donor ability of these molecules is significantly increased with respect to their cationic analogues (Fig. 1, **B**).[12,13]

We have also synthesized neutral triphosphenium molecules with the initial aim of targeting the generation of macrocycles and oligomers for use as multidentate donors (Fig. 1, C). We demonstrated that these molecules could coordinate coinage metals in a bidentate P,P' fashion[14] but we remained intrigued by the possibility of engaging the negatively charged bridging moiety for additional coordination. In particular, we reasoned that the differing electronic behaviour of the potential donor sites in such molecules could allow for differential binding and specificity (e.g. the sites feature both hard and soft donors). Such design elements would permit for the potential generation of multi-metallic systems in which various metals can be selectively coordinated in a controlled manner.

One of the anionic linkers we employed was a cyclopentadienyl (Cp) fragment. Cp ligands are one of the most ubiquitous and coordinatively flexible anionic ligands for transition metals owing to its ability to bind metals in different modes (σ, and η^1 to η^5) and its significant capacity for functionalization. Of particular relevance to the work in this report, it has been demonstrated recently that ferrocene derivatives featuring multiple pendant phosphine groups can bind up to two additional transition metals to generate trimetallic systems, which could prove useful for multi-metallic oligomers or polymers.[15]

With the foregoing design elements in mind, we targeted cyclopentadiene as the backbone of our neutral triphosphenium, with an appended, uncoordinated phosphine at the back (**1**). This could allow for the molecule to function as a 2 e^-, 4 e^- or up to 6 e^- donor, depending on the requirements of the metal to which it binds. The multi-functional nature of the system, which also features a phosphine and a phosphide-like triphosphenium moiety, should also permit for site-specific modification of the parent ligand (e.g. *via* oxidation, protonation and alkylation) for the generation of analogues with different donor abilities. We wish to note that Stradiotto and co-workers demonstrated the practicality of this method in the generation of substituted P,N-indene ligands for transition metals.[16,17] Herein we report a simple method to generate this molecule using a P^I transfer agent and we probe some of the surprising chemistry associated with this multifunctional molecule containing a P^I center.

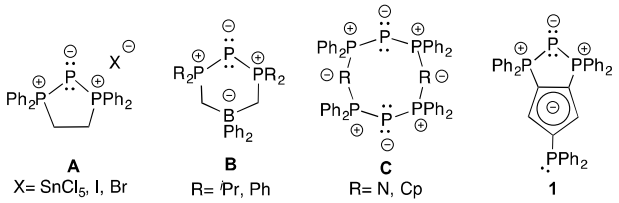

Fig. 1 Selected molecules featuring a triphosphenium fragment, including: triphosphenium cations (**A**) and recent, neutral triphosphenium analogues (**B, C**).

Results and Discussion

Synthesis and characterization of $[(Ph_2P)C_5H_2(Ph_2P)_2P^I]$

The synthesis of our target P^I molecule was inspired by a ligand we have previously commissioned to generate P^I containing macrocycles, namely the potassium salt of 1,3-

[a] Department of Chemistry and Biochemistry, Windsor, Ontario, Canada, N9B 3P4. E-mail: cmacd@uwindsor.ca

Electronic Supplementary Information (ESI) available: NMR spectra and Computational Results. See DOI: 10.1039/x0xx00000x

bis(diphenylphosphino)cyclopentadienide. In order to produce a chelating analogue of these types of molecules, we appended an additional diphenylphosphine fragment to provide 1,2,4-tris(diphenylphosphino)cyclopentadiene, which was deprotonated with potassium hexamethyldisilazide to generate the potassium salt in good yield. The reaction of this potassium tris(diphenylphosphino)cyclopentadiene in a 1:1 stoichometric ratio with [dppeP][Br] yields **1** in quantitative yield (Scheme 1). As anticipated, the presence of two phosphines alpha to each other favors the generation of a monomeric, chelated triphosphenium analogue rather than producing dimers (or higher oligomers)[14]. The $^{31}P\{^{1}H\}$ NMR spectrum of the reaction mixture features singlet, doublet and triplet resonances indicative of **1** (δ 32.4, -16.9, -174.2 ppm respectively, Fig S1) in addition to a singlet for the dppe that is liberated in the process. The crude mixture was filtered to remove KBr and the filtrate was collected and washed with diethyl ether to remove the diphenylphosphinoethane.

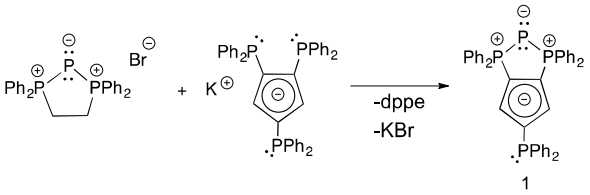

Scheme 1. Synthetic route to a neutral triphosphenium, **1** via ligand metathesis

Crystals of the air-sensitive **1** suitable for X-ray diffraction were obtained from the slow evaporation of a concentrated dichloromethane solution. The molecular structure (Fig. 2) reveals a zwitterionic triphosphenium analogue, crystalizing in the space group $P2_1/c$ with one molecule present in the asymmetric unit. The P-P bond lengths of the triphosphenium fragment, 2.1418(12) and 2.1467(12) Å are relatively long – falling outside of the range of distances reported for cationic cyclic triphosphenium cations (2.11-2.13 Å)[4] – and are most similar to those in Ragogna's zwitterionic triphosphoniums (2.1328(9) to 2.1371(9) Å). Similarly, the P-P^{I}-P angle of 90.39(4)º is obtuse in comparison to typical angles for reported 5-membered ring triphosphenium cations (86-88º). As anticipated, the P-C^{Cp} bond length of the free phosphine (1.802(3) Å) is significantly longer than the P-C^{Cp} distances (1.749(3)-1.750(3) Å) to the chelating phosphine groups.

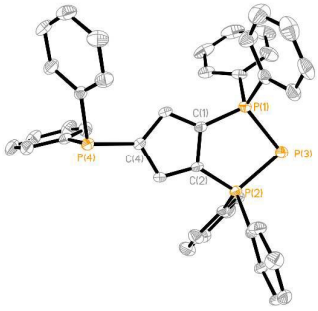

Fig. 2 Thermal ellipsoid plot of **1.** Ellipsoids are drawn at 50% probability and hydrogen atoms are removed for clarity. Selected bond distances (Å) and angles (º): P1-P3: 2.1418(12), P2-P3: 2.1467(12) P1-C1: 1.750(3), P2-C2: 1.749(3), P4-C4: 1.802(3), P1-P3-P2: 90.39(4).

We conducted cyclic voltammetry (CV) experiments as a preliminary probe for the reactivity of the three potential sites of this ligand. The groups of Alcarazo,[18] Weigand[19] and ourselves[20] have previously employed this technique to attempt to quantify the donating ability of ligands containing a low valent phosphorus atom. The voltammogram for compound **1** (Fig. 3) shows both quasi-reversible and irreversible oxidation peaks at potentials of +0.227 V and +0.817 V (versus Fc/Fc^{+}).

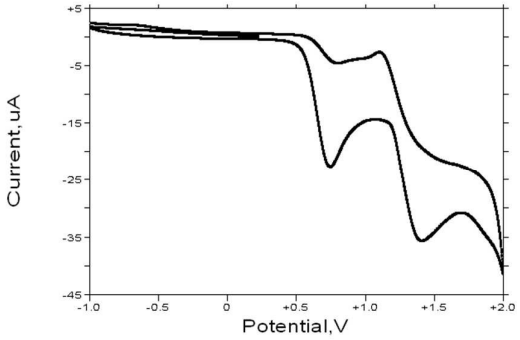

Fig. 3 Cyclic voltammogram of **1** showing irreversible and quasi-reversible oxidation peaks; the potential illustrated is with respect to Ag/AgCl(1M).

On the basis of the CV data obtained for both starting materials (Fig S14, S15) we postulate that the potentials correspond to two oxidations; the lower one likely being attributable to the cyclopentadienyl ring and the higher one being attributable to the P^{I} center (cf. the oxidation potential of $[(dppe)P]^{+}$ at 1.066 V (Fig S15)). The latter assignment suggest that **1** should be a better donor than the triphosphenium cation found in the starting material and investigated previously.[12]

Coordination of AuCl to $[(Ph_2P)C_5H_2(Ph_2P)_2P^{I}]$

In order to probe the ligand properties of our zwitterionic triphosphenium with transition metals, we selected to conduct our initial investigation using d^{10} coinage metals as these have been found to coordinate to various low valent centers and the linear structures minimize steric complications.[13,14,21] We found that the addition of an orange suspension of gold(I) chloride to a stirring bright yellow solution of **1** resulted in an immediate colour change from yellow to gold. The reaction was monitored by $^{31}P\{^{1}H\}$ NMR, and the most obvious change in the spectrum of the reaction mixture is a significant deshielding of the singlet signal corresponding to the terminal phosphine to 25 ppm (cf. -16.9 ppm in **1**) (Fig. S3). This observation suggested that the gold (I) chloride coordinates through the appended phosphine rather than at the P^{I} center (Scheme 3). This perhaps unanticipated result is confirmed by the molecular structure obtained from crystals grown from a concentrated solution of dichloromethane.

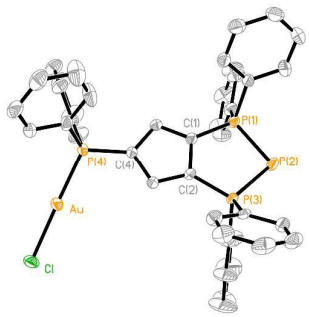

Fig. 4 Thermal ellipsoid plot of 2, hydrogen atoms omitted for clarity and ellipsoids drawn at 50% probability. Selected bond distances (Å) and angles (º): P1-P2: 2.1377(10) P2-P3: 2.1378(10) P1-C1: 1.760(3) P3-C2: 1.767(3) P4-C4: 1.7808(3) P1-P3-P2: 91.09(4)

The molecule crystalizes in the space group P $2_1/c$ with one molecule present in the asymmetric unit (Fig. 4). Notably, the P-Au distance of 2.2336(7) Å falls within the typical range of AuCl fragments bound to phosphine ligands in the Cambridge Structural Database (CSD).[22] Additionally, there is a significant decrease in the bond length of the phosphine to the carbon of the cyclopentadienyl group to 1.780(3) Å (*cf.* 1.802 Å in **1**). Preliminary NMR studies of reactions with 2:1 stoichiometric ratio of gold suggest that the second equivalent of gold is indeed bound at the P^I center.

Protonation Reactions of $[(Ph_2P)C_5H_2(Ph_2P)_2P^I]$

In light of the perhaps surprising result with gold(I), we investigated reactions with a strong main group acceptor – a proton – to further probe the reactivity of this molecule. Again to our surprise, the addition of trifluoromethanesulfonic (triflic) acid protonates selectively, at the pendant phosphine when added in a 1:1 ratio (Scheme 2). This is indicated by a significant, downfield shift of the singlet corresponding to the terminal phosphine from -17 ppm to -4 ppm while the doublet and triplet signals corresponding to the triphosphenium fragment remain at the nearly the same shifts. (Figure 5, **B**).

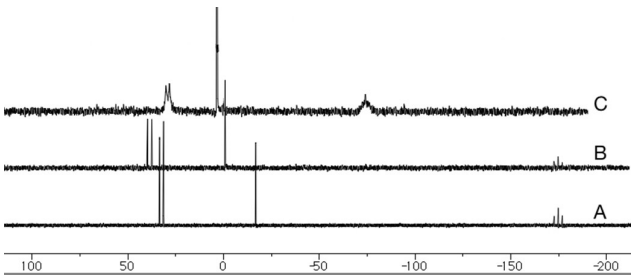

Fig. 5 $^{31}P\{^1H\}$ NMR spectra of **1** (A) and its reactions with HOTf (B), and 2 eq. HOTf, (C).

Thus it appears as if not only soft Lewis acids, such as gold(I) chloride, selectively react at the terminal phosphine, but so do harder acids. Based on ^{31}P NMR investigations, the

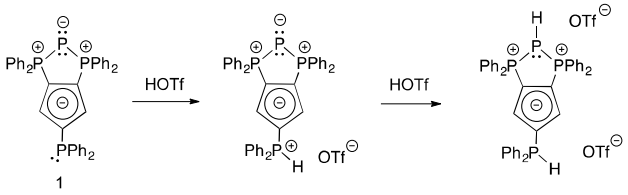

addition of a further equivalent of triflic acid protonates the P^I center, shifting the corresponding triplet peak from -178 ppm to *ca*. -80 ppm (Figure 5, **C**). Unfortunately, we have as of yet been unsuccessful in obtaining high-quality single crystals for the protonated products.

Scheme 2. Reaction of **1** with 1 and 2 eq. triflic acid, respectively and propsed products

Computational Investigations

The observation that the **1** binds at the tricoordinate phosphine (P^{III}) site rather than the dicoordinate phosphide-like (P^I) site suggested that an overly simple model of electron density – i.e. one based on canonical forms of Lewis-type drawings such as in Fig. 1 – does not provide accurate predictions of reactivity. In order to obtain a more accurate understanding of the electronic structure and reactivity of compounds such as **1**, we conducted a series of density functional theory (DFT) calculations using the M062X/TZVP approach. The results of these calculations are particularly enlightening. Geometry optimization of a complete model of **1** bearing phenyl substituents accurately reproduces all of the structural features observed experimentally but the calculations are computationally expensive. We found that a model complex in which all of the phenyl substituents are modelled with hydrogen atoms ($[(H_2P)_3(C_5H_2)P^I]$, **1'**) also provides excellent agreement with the experimental observations (see the Supporting Information) at a much lower computational cost; this model was used for the more in-depth computational reactivity investigations.

Interestingly, examination of the frontier molecular orbitals for **1'** (Fig. 6) reveals that the three highest energy occupied molecular orbitals (HOMO to HOMO-2) are all primarily based on either the triphosphenium fragment or the cyclopentadienyl fragment! In fact, the HOMO (and LUMO) is very similar in composition to those of other cyclic triphosphenium ions.[23] Thus one might predict that **1'** should function as a donor either via the P^I center or the Cp fragment. In fact, the orbital corresponding to the "lone pair" on the free phosphine fragment – the fragment that actually appears to react in the experimental observations – is HOMO-3 and is around 1 eV more stable than the HOMO.

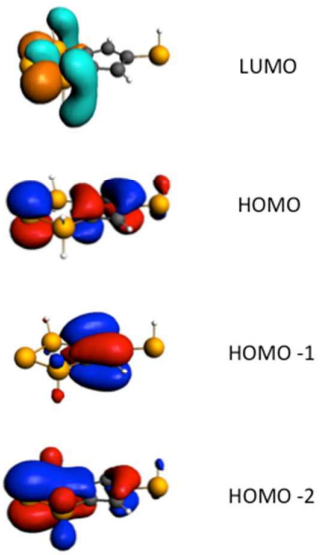

Fig. 6 Depictions of the frontier orbitals of **1'.**

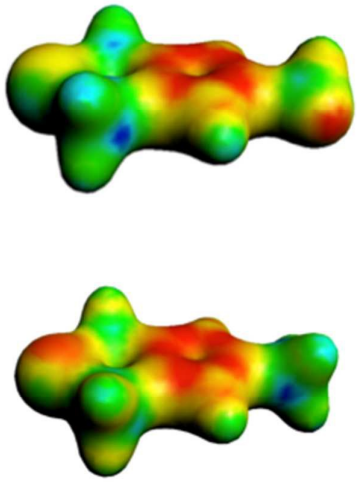

Fig. 7 Electrostatic potential map of **1'** (above) and protonated variant (below); regions colored red exhibit the highest potentials and regions in violet have the lowest potentials.

Given that the simple frontier MO analysis also did not appear to provide a rationale for the experimental results, we examined the electrostatic potential (ESP) of **1'**. A plot of the ESP of **1'** mapped onto the electron density – illustrated in Fig. 7 (top) – does indeed provide insight into the regiochemistry observed experimentally. The highest potential (depicted in red) on **1'** is localized on the free phosphine fragment; there is a somewhat smaller potential localized on the Cp ring and a considerably decreased potential on the P^{I} fragment. This observation suggests that, perhaps in contrast to simple chemical intuition, the phosphine fragment should indeed be the most reactive part of the molecule.

Calculations of the proton affinities for **1'** for binding a proton at either the P^{I} or P^{III} sites reveal that the binding of a proton at the tricoordinate phosphine site is 36 kJ mol^{-1} more favourable than is binding a proton at the dicoordinate P^{I} site. Interestingly, the calculations predict that protonation at the Cp ring is even more favourable (but by less than 3 kJ mol^{-1}) for this model but we see no evidence of such chemistry experimentally. Thus the proton binding calculations corroborate the conclusions drawn from the ESP calculations and the experimental observations in terms of the preference of the site of phosphorus reactivity.

Importantly, examination of the ESP of the most stable protonated variant of **1'** (i.e. $\mathbf{[P(H_2P)_2C_5H_2PH_3]^+}$) reveals that protonation of the phosphine results in a cation in which the P^{I} center and the Cp ring have a high potential (Fig. 7, bottom). This observation suggests that the ligand properties of **1**, should indeed be tunable using acids.

Similarly, calculations of the electrostatic potentials of derivatives of **1'** in which the phosphine is protected with oxygen, sulfur, borane, and methyl groups (see Supporting Information) suggest that the binding properties and preferences of these variants may be easily modified.

Reaction of $[(Ph_2P)C_5H_2(Ph_2P)_2P^{I}]$ and elemental sulfur

With the results of our computational investigation in hand, we sought to selectively react the terminal phosphine with a chalcogen in order to evaluate how the properties of the compound change in particular regard to the cyclopentadienyl or P^{I} moiety. The addition of a yellow solution of **1** in dichloromethane to a suspension of one equivalent of sulfur in dichloromethane results in immediate reaction that yields a cloudy yellow solution. The reaction is complete after 10 minutes and can be monitored by $^{31}P\{^{1}H\}$ NMR spectroscopy: once again, there was a significant shielding (from δ -16.9 ppm to δ 35.4 ppm) of the singlet corresponding to the terminal phosphine while the doublet and triplet (δ 35 ppm, -173 ppm) attributable to the triphosphenium fragment, are virtually unchanged from their original shifts (*cf.* δ 34 ppm, -175 ppm). The NMR spectroscopy is again consistent with the reaction having occurred at the appended phosphine moiety. (Scheme 3). The product can be obtained from simply removing the reaction solvent (dichloromethane), as the product is generated in quantitative yield. The moderately- air sensitive solid can be stored indefinitely in an inert atmosphere and is stable for several hours on the bench top without decomposition.

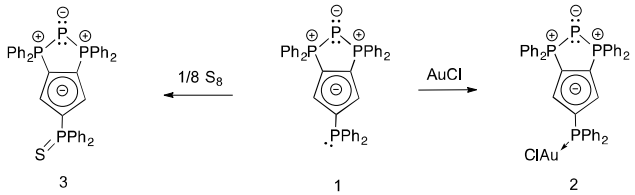

Scheme 3. Reaction of **1** with elemental sulfur and gold chloride respectively

The regiochemistry of the reaction to generate the sulfide **3** inferred on the basis of the NMR spectroscopy was confirmed by the molecular structure obtained from crystals grown from dichloromethane. The molecule crystalizes in the space group $P2_1/c$ with one molecule present in the asymmetric unit (Fig. 8). The P-S bond length is 1.9618(10) Å and is well within the range of phosphine sulfide bond lengths reported in the CSD[22]. As anticipated, there is a significant shorting of the P-C^{Cp} bond distance to 1.778(3) Å (*cf.* 1.802(3) Å) in comparison to the parent ligand. The bond lengths within the triphosphenium moiety virtually unchanged in the thionated ligand.

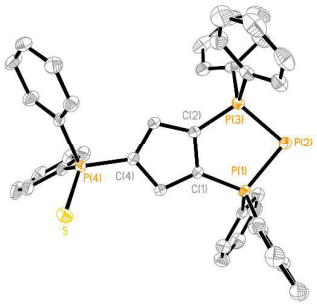

Fig. 8 Thermal ellipsoid plot of **3**, hydrogen atoms omitted for clarity and ellipsoids drawn at 50% probability. Selected bond distances (Å) and angles (º): P1-P2: 2.1477(10), P2-P3: 2.1393(10) P1-C1: 1.763(3), P3-C2: 1.757(3), P4-C4: 1.778(3), P1-S: 1.9618(10) P1-P3-P2: 90.8(4).

In order to evaluate the changes in the redox properties, we also conducted cyclic voltammetry experiments on **3** in order to compare the results to those of the parent molecule(Fig. 9). We found that there is only one clear oxidation potential present, which corresponds to an irreversible oxidation appearing at 0.662 V (versus Fc/Fc^+) which appears to overlap with an oxidation at higher potential (ca. 0.9 V).

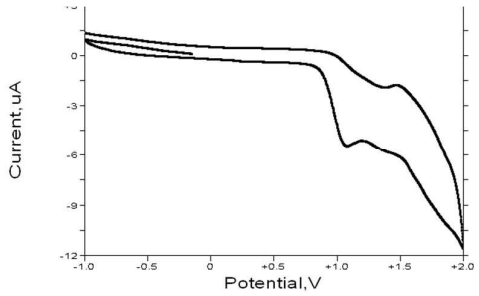

Fig. 9 Cyclic Voltammogram of 3 showing two overlapping oxidation peaks; the potential illustrated is with respect to Ag/AgCl (1M).

Thus it appears as if the alteration of the relatively electron-donating PPh_2 fragment in **1** to a much more electron-withdrawing $P(S)Ph_2$ fragment in **3** to results in a significant increase in the oxidation potential of the Cp ring, as one would anticipate.

Conclusions

In conclusion, we report a new multifunctional zwitterionic triphosphenium and have provided some insight into its reactivity. Both reactivity studies and calculations reveal that this molecule is most reactive at the phosphine fragment rather than at the P^I fragment. In particular, experimental investigations reveal that the reaction of **1** with gold(I), protons, or sulfur all result in selective binding at the free phosphine initially. Computational investigations suggest that this ligand can easily be modified to preferentially bind at either the cyclopentadienyl ring or the P^I moiety, by blocking the terminal phosphine. Experiments to probe the reactivity of **1** with many other transition metal fragments are underway and efforts to generate derivatives of this molecule are on-going. It is anticipated that other derivatives and analogues featuring alkyl phosphine substituents or with other kinds of substitution on the Cp ring should allow for the generation of complexes that are bound at each of the possible donor sites.

Experimental

All manipulations were carried out using standard inert atmosphere techniques. All chemicals and reagents were purchased from Sigma-Aldrich and used without further purification. Deuterated solvents were dried according to literature procedure when necessary, and all other solvents were dried over a series of Grubbs'-type columns and degassed prior to use. The ligand, $[K][(Ph_2P)_3C_5H_2]$ was synthesized according to modified literature procedures[14,15]. NMR spectra were recorded at room temperature on a Bruker Avance III 500 MHz or Bruker Avance Ultrashield 300 spectrometer. Chemical shifts are reported in ppm relative to internal standards for ^1H and ^{13}C (the given deuterated solvent) and external standards for and ^{31}P (85% H_3PO_4). Coupling constants |J| are given in Hz, Elemental Analysis was performed at the University of Windsor using a Perkin Elmer 2400 combustion CHN analyser. Cyclic voltammetry was performed in dry CH_2Cl_2 solutions using $[NBu_4][PF_6]$ (0.1 M) as the electrolyte with analyte concentration of approximately 0.01 M. A glassy carbon electrode, a platinum wire, and 1.0M Ag/AgCl electrode were used as the working, auxiliary, and reference electrodes, respectively. The experiments were run with a scan rate of 100mV/s and a sensitivity of 100 µA/V and the potentials reported are referenced to ferrocene/ferrocenium ($E^1/_2$ = 0.0 V).

Computational Details

All of the computational investigations were performed using the Compute Canada Shared Hierarchical Academic Research Computing Network (SHARCNET) facilities (www.sharcnet.ca) with the Gaussian09[24] program suites. Geometry optimizations have been calculated using density functional theory (DFT), specifically implementing the M062X method[25] in conjunction with the TZVP basis set[26] for all atoms. The geometry optimizations were not subjected to any symmetry restrictions

and each stationary point was confirmed to be a minimum having zero imaginary vibrational frequencies. Pictures of the optimized structures were prepared using Gaussview 3.0.[27] Population analyses were conducted using the Natural Bond Orbital (NBO)[28] implementation included with the Gaussian package. Plots of molecular orbitals and electrostatic potentials were generated at the M062X\TZVP level of theory and examined using ADF2014.[29–31] Summaries of the optimized structures, including electronic energies and Cartesian components for each of the atoms, are detailed in supplementary information.

Crystallographic Details

Crystals for investigation were covered in Nujol®, mounted into a goniometer head, and then rapidly cooled under a stream of cold N_2 of the low-temperature apparatus (Oxford Cryostream) attached to the diffractometer. The data were then collected using the APEXII software suite[32] on a Bruker Photon 100 CMOS diffractometer or using the SMART software on a Bruker APEX CCD diffractometer using a graphite monochromator with MoK_α radiation (λ = 0.71073 Å). For each sample, data were collected at low temperature. APEXII software was used for data reductions and SADABS[33] was used for absorption corrections (multi-scan; semi-empirical from equivalents). XPREP was used to determine the space group and the structures were solved and refined using the SHELX[34] software suite as implemented in the WinGX[35] program suites. Validation of the structures was conducted using PLATON.[36] Details are provided in Table 1.

Specific Procedures

Synthesis of $[(Ph_2P)C_5H_2(Ph_2P)_2P^I]$ (1). To a cold, stirring white suspension of [dppeP][Br] (1.939g, 3.8 mmol) in THF was added a THF solution of $[K][(Ph_2P)_3C_5H_2]$ (2.50g, 3.8 mmol). Upon addition, the solution was allowed to warm to room temperature and a yellow colour appeared with the production of a white precipitate. The solution was subsequently filtered through Celite® and washed with THF (10 mL) to remove KBr and the yellow filtrate was collected. The THF was removed from the filtrate *in vacuo* to obtain a bright yellow powder. This powder was washed with a 60:40 pentane:diethyl ether mixture (2 x 40 mL) and the subsequent bright yellow precipitate was collected as **1.** (2.24g 91%) **$^{31}P\{^1H\}$ NMR** (CD_2Cl_2): δ 32.4 (d, $^1J_{P-P}$ = 426 Hz), -16.9 (s), -174.22 (t, $^1J_{P-P}$ = 426 Hz); **^1H NMR** (CD_2Cl_2): δ 7.77-7.2 (m, 30 H, Ar), 6.57 (*pseudo-q* $^2J_{P-H}$= 3.5 Hz, $^3J_{P-H-}$=3.5 Hz, 2H, C_5H_2); **$^{13}C\{^1H\}$ NMR** (CD_2Cl_2) δ 141.7 (d, $^1J_{PC}$ = 10.4 Hz, Ph); 133.5 (d, $^1J_{PC}$ = 7 Hz, P-C^{Cp}); 133.0 (d, 18.6 Hz, Ph); 132.5(d, 7.3 Hz, P-C^{Cp}); 131.9 (d, 10.7 Hz, Ph), 131.4 (s, *para*-Ph); 128.7 (d, 12 Hz, Ph); 127.9 (d, 5.6 Hz, Ph); 127.5 (s, *para*-Ph); 121.5 (m, $^2J_{PC}$ ≈ 5 Hz, C^{Cp}-H). Anal. Calcd for $C_{41}H_{32}P_4N$: C, 73.93; H, 4.97; N, 0; found: C, 73.61; H, 4.93; N,-0.05%. HR-ESI-MS: calcd for $[C_{41}H_{32}P_4]$+ m/z = 648.1460, found: 648.1455

Crystals were obtained via slow evaporation from a concentrated solution of dichloromethane.

Synthesis of $[(Ph_2P(AuCl))C_5H_2(Ph_2P)_2P^I]$ (2).

To a stirring pale yellow solution of $[(Ph_2P)C_5H_2(Ph_2P)_2P^I]$ (**1**) (0.110g, 0.169 mmol) was added a dichloromethane suspension of AuCl (0.039g, 0.169 mmol). Upon addition, the solution turned a golden yellow colour and was allowed to stir for 10 minutes. The dichloromethane was removed and the subsequent yellow powder was washed with diethyl ether (5 mL) and then collected. (0.141g, 94.6%) **$^{31}P\{^1H\}$ NMR (CD_2Cl_2):** δ 34.11 (d, $^1J_{P-P}$ = 404.9 Hz), 18.7 (s), -175.0 (t, $^1J_{P-P}$ = 432 Hz); **^1H NMR (CD_2Cl_2):** δ 7.72-7.33 (m, 30 H, Ar), 6.67 (*pseudo-q* $^2J_{P-H}$= 3.5 Hz, $^3J_{P-H-}$=3.5 Hz, 2H, C_5H_2); δ **Anal. Calcd** for $C_{41}H_{32}P_4AuCl$: C, 55.9; H, 3.66; N, 0; found: C, 55.77; H, 3.70; N,-0.05%.

Crystals were obtained via slow evaporation from a concentrated solution of dichloromethane.

Synthesis of $[(Ph_2P(S))C_5H_2(Ph_2P)_2P^I]$ (3).

To a stirring pale yellow solution of $[(Ph_2P)C_5H_2(Ph_2P)_2P^I]$ (**1**) (0.189g, 0.29 mmol) was added a dichloromethane suspension of elemental sulfur (0.009g, 0.036mmol) There was no colour change upon addition and the solution was allowed to stir for 1 hour at which point solution was centrifuged to ensure no unreacted sulphur remained, and the resulting solution was collected. Dichloromethane was removed and the subsequent pale yellow powder was collected (0.191g 97%) **$^{31}P\{^1H\}$ NMR** (CD_2Cl_2): δ 35.3 (d, $^1J_{P-P}$ = 431.2 Hz), 35.38 (s), -173.3 (t, $^1J_{P-P}$ = 430.9 Hz); **^1H NMR** (CD_2Cl_2): δ 7.70-7.3 (m, 30 H, Ph), 6.57 (*pseudo-q* $^2J_{P-H}$= 4.75 Hz, $^3J_{P-H-}$= 4.75 Hz, 2H, C_5H_2); **$^{13}C\{^1H\}$ NMR** (CD_2Cl_2) δ 137.2 (s, Ph); 136.1 (s, Ph); 132.60 (d, $^1J_{C-P}$ unresolved, C^{CP}-P); 132.60-131.75 (m, $^2J_{PC}$ ≈12.45 Hz, Ph); 130.5 (s, C^{Cp}-H); 128.8 (d, $^2J_{PC}$= 12.5 Hz, Ph); 128.0(d, $^2J_{PC}$= 12.2 Hz), 120.5 (m, $^2J_{PC-}$ unresolved C^{CP}-P)

Anal. Calcd for $C_{41}H_{32}P_4S$: C, 72.35; H, 4.74; N, O; found: C, 72.05; H, 4.61; N, 0.1.

Crystals were obtained via slow evaporation from a concentrated solution of dichloromethane.

Acknowledgements

We thank the Natural Sciences and Engineering Research Council (NSERC) of Canada and the Canada Foundation for Innovation (CFI) for funding and equipment.

Notes and References

1 T. Chivers and J. Konu, *Comments Inorg. Chem.*, 2009, **30**, 131–176.

2 C. L. B. Macdonald, B. D. Ellis and A. Swidan, in *Encyclopedia of Inorganic and Bioinorganic Chemistry*, John Wiley & Sons, Ltd, 2011.

3 B. D. Ellis and C. L. B. Macdonald, *Coord. Chem. Rev.*, 2009, **253**, 2783.

4 P. K. Coffer (née Monks) and K. B. Dillon, *Coord. Chem. Rev.*, 2013, **257**, 910–923.

5 B. D. Ellis and C. L. B. Macdonald, *Inorg. Chem.*, 2006, **45**, 6864–74.

6 E. L. Norton, K. L. S. Szekely, J. W. Dube, P. G. Bomben and C. L. B. Macdonald, *Inorg. Chem.*, 2008, **47**, 1196–1203.

7 P. K. Coffer née Monks, R. M. K. Deng, K. B. Dillon, M. a Fox and R. J. Olivey, *Inorg. Chem.*, 2012, **51**, 9799–808.

8 S. Klein, R. Tonner and G. Frenking, *Chem. - A Eur. J.*, 2010, **16**, 10160–70.

9 R. Corberán, S. Marrot, N. Dellus, N. Merceron-Saffon, T. Kato, E. Peris and A. Baceiredo, *Organometallics*, 2009, **28**, 326–330.

10 M. Alcarazo, C. W. Lehmann, A. Anoop, W. Thiel and A. Fürstner, *Nat. Chem.*, 2009, **1**, 295–301.

11 S. Khan, G. Gopakumar, W. Thiel and M. Alcarazo, *Angew. Chemie - Int. Ed.*, 2013, **52**, 5644–5647.

12 J. W. Dube, C. L. B. Macdonald, B. D. Ellis and P. J. Ragogna, *Inorg. Chem.*, 2013, **52**, 11438–49.

13 J. W. Dube, C. L. B. Macdonald and P. J. Ragogna, *Angew. Chem. Int. Ed. Engl.*, 2012, **51**, 13026–30.

14 S. C. Kosnik, G. J. Farrar, E. L. Norton, B. F. T. Cooper, B. D. Ellis and C. L. B. Macdonald, *Inorg. Chem.*, 2014, **11**, 13061–13069.

15 R. V. Smaliy, M. Beaupérin, A. Mielle, P. Richard, H. Cattey, A. N. Kostyuk and J. C. Hierso, *Eur. J. Inorg. Chem.*, 2012, 1347–1352.

16 M. Stradiotto, J. Cipot and R. Mcdonald, *J. Am. Chem. Soc.*, 2003, 5618–5619.

17 J. Cipot, C. M. Vogels, R. McDonald, S. a. Westcott and M. Stradiotto, *Organometallics*, 2006, **25**, 5965–5968.

18 M. Alcarazo, *Chem. - A Eur. J.*, 2014, **20**, 7868–7877.

19 K. Schwedtmann, S. Schulz, F. Hennersdorf, T. Strassner, E. Dmitrieva and J. J. Weigand, *Angew. Chemie Int. Ed.*, 2015, **54**, 11054–11058.

20 J. F. Binder, A. Swidan, M. Tang, J. H. Nguyen and C. L. B. Macdonald, *Chem. Commun.*, 2015, **51**, 7741–7744.

21 K. Schwedtmann, M. H. Holthausen, K.-O. Feldmann and J. J. Weigand, *Angew. Chem. Int. Ed. Engl.*, 2013, **52**, 14204–8.

22 F. H. Allen, *Acta Crystallogr. Sect. B Struct. Sci.*, 2002, **58**, 380–388.

23 B. D. Ellis and C. L. B. Macdonald, *Inorg. Chem.*, 2006, **45**, 6864–6874.

24 M. J. Frisch, G. W. Trucks, H. B. Schlegel, G. E. Scuseria, M. A. Robb, J. R. Cheeseman, G. Scalmani, V. Barone, B. Mennucci, G. A. Petersson, H. Nakatsuji, M. Caricato, X. Li, H. P. Hratchian, A. F. Izmaylov, J. Bloino, G. Zheng, J. L. Sonnenberg, M. Hada, M. Ehara, K. Toyota, R. Fukuda, J. Hasegawa, M. Ishida, T. Nakajima, Y. Honda, O. Kitao, H. Nakai, T. Vreven, J. A. Montgomery Jr., J. E. Peralta, F. Ogliaro, M. Bearpark, J. J. Heyd, E. Brothers, K. N. Kudin, V. N. Staroverov, R. Kobayashi, J. Normand, K. Raghavachari, A. Rendell, J. C. Burant, S. S. Iyengar, J. Tomasi, M. Cossi, N. Rega, J. M. Millam, M. Klene, J. E. Knox, J. B. Cross, V. Bakken, C. Adamo, J. Jaramillo, R. Gomperts, R. E. Stratmann, O. Yazyev, A. J. Austin, R. Cammi, C. Pomelli, J. W. Ochterski, R. L. Martin, K. Morokuma, V. G. Zakrzewski, G. A. Voth, P. Salvador, J. J. Dannenberg, S. Dapprich, A. D. Daniels, Ö. Farkas, J. B. Foresman, J. V Ortiz, J. Cioslowski and D. J. Fox, *Gaussian Inc Wallingford CT*, 2009, 34, Wallingford CT.

25 Y. Zhao and D. G. Truhlar, *Theor. Chem. Acc.*, 2008, **120**, 215–241.

26 A. Schäfer, C. Huber and R. Ahlrichs, *J. Chem. Phys.*, 1994, **100**, 5829–5835.

27 Gaussian Inc, *Gaussview 3.0, (2003) Gaussian Inc., Pittsburgh, PA.*, Pittsburgh, PA., 2003.

28 A. E. Reed, L. A. Curtiss and F. Weinhold, *Chem. Rev.*, 1988, **88**, 899–926.

29 G. Te Velde, F. M. Bickelhaupt and S. J. A. Gisbergen, *J. Comput. Chem*, 2001, **22**, 931–967.

30 E. J. Baerends, A. Bérces, C. Bo, P. M. Boerringter, L. Cavallo, L. Deng, R. M. Dickson, D. E. Ellis, L. Fan and T. H. Fischer, *Theor. Chim. Acta*, 1998, **99**, 391.

31 T. N. ADF 2014, (2014) SCM, Theoretical Chemistry, Vrije Universiteit, Amsterdam, .

32 APEX II. Bruker AXS Inc., Madison, WI, 2012.

33 SADABS, *Bruker AXS, Madison, Wi*, 2001.

34 G. . Sheldrick, 2001.

35 L. J. Farrugia, *J. Appl. Crystallogr.*, 1999, 32, 837–838.

36 A. L. Spek, *J. Appl. Crystallogr.*, 2003, **36**, 7–13.

Table 1: Summary of Crystallographic Data

Compound	**[(Ph$_2$P)C$_5$H$_2$(Ph$_2$P)$_2$P^I]**	**[(Ph$_2$P(AuCl))C$_5$H$_2$(Ph$_2$P)$_2$P^I]**	**[(Ph$_2$P(S))C$_5$H$_2$(Ph$_2$P)$_2$P^I]**
CCDC ID	1429515	1429516	1429517
Empirical formula	$C_{41}H_{32}P_4$	$C_{41}H_{32}P_4AuCl$	$C_{41}H_{32}P_4S$
Formula weight	648.54	880.96	680.60
Temperature/K	173(2)	173(2)	173(2)
Crystal system	Monoclinic	Monoclinic	Monoclinic
Space group	*P 2$_1$/c*	*P 2$_1$/c*	*P 2$_1$/c*
a/Å	9.0352(3)	13.5468(5)	8.9112(2)
b/Å	14.2222(3)	16.8119(5)	14.6975(4)
c/Å	26.5598(8)	16.3995(6)	26.2859(6)
α/°	90	90	90
β/°	98.9630(10)	106.8580(10)	98.2890(10)
γ/°	90	90	90
Volume/Å^3	3371.27(17)	3574.4(2)	3406.76(14)
Z	4	4	4
ρ_{calc}g/cm^3	1.278	1.637	1.327
μ/mm^{-1}	0.253	4.399	2.841
F(000)	1352	1736	1416
Crystal size/mm^3	0.198 × 0.138 × 0.125	0.242× 0.161 × 0.093	0.185 × 0.129 × 0.040
2Θ range for data collection/°	2.901 to 26.416	2.749 to 27.495	3.398 to 74.675
Index ranges	-11 ≤ h ≤ 11, -17 ≤ k ≤ 17, -33 ≤ l ≤ 33	-17 ≤ h ≤ 17, -21≤ k ≤ 21, -21≤ l ≤ 21	-11 ≤ h ≤ 9, -18 ≤ k ≤ 18, -32≤ l ≤ 32
Reflections collected	55110	151199	56406
Independent reflections	6904[R_{int} = 0.2284]	8200 [R_{int} = 0.0343]	6930 [R_{int} = 0.1059]
Data/restraints/parameters	6904/ 0 / 406	8200/ 0 / 426	6930/ 0 / 417
Goodness-of-fit on F2	1.035	1.096	1.046
Final R indexes [I>=2σ (I)]	R_1 = 0.0574 wR_2 = 0.1161	R_1 = 0.0247 wR_2 = 0.0558	R_1 = 0.0492 wR_2 = 0.1200
Final R indexes [all data]	R_1 = 0.1152 wR_2 = 1.1431	R_1 = 0.0300, wR_2 = 0.0595	R_1 = 0.0723, wR_2 = 0.1325
Largest diff. peak/hole / e Å-3	0.369/-0.509	1.770/-2.540	0.533/-0.387
Refinement method		Full-matrix least-squares on F^2	
Data completeness	0.999	0.998	0.995

$R_1 = \Sigma(\ |Fo| - |Fc|\ ) / \Sigma F_o$, $wR2 = [\ \Sigma(\ w(\ F_o^2 - F_c^2)^2\ ) / \Sigma(wF_o^4\ )\ ]$., GOF = $[\Sigma(w(F_o^2-F_c^2)^2) / (\text{No. of reflns. - No. of params.})]^{1/2}$.

Graphical Abstract

We present a zwitterionic triphosphenium molecule which features dicoordinate, tricoordinate and tetracoordinate phosphorus centers in addition to a cyclopentadienyl moiety. Crystallographic, computational, electrochemical and spectroscopic data illustrate and rationalize the reactivity of this molecule as a multifunctional ligand for both transition metals and main group acceptors and suggest how the donor properties may be tuned.